

Three key regimes of single pulse generation per round trip of all-normal-dispersion fiber lasers mode-locked with nonlinear polarization rotation

Sergey Smirnov,^{1,*} Sergey Kobtsev,¹ Sergey Kukarin,¹ and Aleksey Ivanenko^{1,2}

¹Division of Laser Physics and Innovative Technologies, Novosibirsk State University, 630090, Novosibirsk, Russia

²Aston Institute of Photonic Technologies, Aston University, Birmingham, B4 7ET, UK

*smirnov@lab.nsu.ru

Abstract: We show experimentally and numerically new transient lasing regime between stable single-pulse generation and noise-like generation. We characterize qualitatively all three regimes of single pulse generation per round-trip of all-normal-dispersion fiber lasers mode-locked due to effect of nonlinear polarization evolution. We study spectral and temporal features of pulses produced in all three regimes as well as compressibility of such pulses. Simple criteria are proposed to identify lasing regime in experiment.

©2012 Optical Society of America

OCIS codes: (140.4050) Mode-locked lasers; (140.3510) Lasers, fiber; (140.7090) Ultrafast lasers.

References and links

1. A. Chong, W. H. Renninger, and F. W. Wise, "Properties of normal-dispersion femtosecond fiber lasers," *J. Opt. Soc. Am. B* **25**(2), 140–148 (2008).
2. F. W. Wise, A. Chong, and W. H. Renninger, "High-energy femtosecond fiber lasers based on pulse propagation at normal dispersion," *Laser Photon. Rev.* **2**(1-2), 58–73 (2008).
3. V. L. Kalashnikov, E. Podivilov, A. Chernykh, and A. Apolonski, "Chirped-pulse oscillators: theory and experiment," *Appl. Phys. B* **83**(4), 503–510 (2006).
4. S. Kobtsev, S. Kukarin, and Yu. Fedotov, "Ultra-low repetition rate mode-locked fiber laser with high-energy pulses," *Opt. Express* **16**(26), 21936–21941 (2008).
5. P. Grellu and N. Akhmediev, "Dissipative solitons for mode-locked lasers," *Nat. Photonics* **6**(2), 84–92 (2012).
6. A. Komarov, H. Leblond, and F. Sanchez, "Multistability and hysteresis phenomena in passively mode-locked fiber lasers," *Phys. Rev. A* **71**(5), 053809 (2005).
7. D. Mao, X. Liu, L. Wang, H. Lu, and L. Duan, "Coexistence of unequal pulses in a normal dispersion fiber laser," *Opt. Express* **19**(17), 16303–16308 (2011).
8. B. Oktem, C. Ülğüdü, and Ö. Ilday, "Soliton-similariton fibre laser," *Nat. Photonics* **4**(5), 307–311 (2010).
9. X. Liu, "Numerical and experimental investigation of dissipative solitons in passively mode-locked fiber lasers with large net-normal-dispersion and high nonlinearity," *Opt. Express* **17**(25), 22401–22416 (2009).
10. C. Lecaplain, Ph. Grellu, J. M. Soto-Crespo, and N. Akhmediev, "Dissipative Rogue-Waves Generated by Chaotic Pulse Bunching in a Mode-Locked Laser," *Phys. Rev. Lett.* **108**(23), 233901 (2012).
11. S. Kobtsev, S. Kukarin, S. Smirnov, S. Turitsyn, and A. Latkin, "Generation of double-scale femto/pico-second optical lumps in mode-locked fiber lasers," *Opt. Express* **17**(23), 20707–20713 (2009).
12. M. Horowitz, Y. Barad, and Y. Silberberg, "Noiselike pulses with a broadband spectrum generated from an erbium-doped fiber laser," *Opt. Lett.* **22**(11), 799–801 (1997).
13. M. Horowitz and Y. Silberberg, "Control of noiselike pulse generation in erbium-doped fiber lasers," *IEEE Photon. Technol. Lett.* **10**(10), 1389–1391 (1998).
14. D. Y. Tang, L. M. Zhao, and B. Zhao, "Soliton collapse and bunched noise-like pulse generation in a passively mode-locked fiber ring laser," *Opt. Express* **13**(7), 2289–2294 (2005).
15. L. M. Zhao, D. Y. Tang, J. Wu, X. Q. Fu, and S. C. Wen, "Noise-like pulse in a gain-guided soliton fiber laser," *Opt. Express* **15**(5), 2145–2150 (2007).
16. L. Wang, X. Liu, Y. Gong, D. Mao, and L. Duan, "Observations of four types of pulses in a fiber laser with large net-normal dispersion," *Opt. Express* **19**(8), 7616–7624 (2011).
17. G. P. Agrawal, *Nonlinear Fiber Optics*, 3rd ed. (Academic Press, 2001).

18. K. Ozgören and F. Ö. İlday, "All-fiber all-normal dispersion laser with a fiber-based Lyot filter," *Opt. Lett.* **35**(8), 1296–1298 (2010).
19. L. Zhao, D. Tang, X. Wu, and H. Zhang, "Dissipative soliton generation in Yb-fiber laser with an invisible intracavity bandpass filter," *Opt. Lett.* **35**(16), 2756–2758 (2010).
20. A. Komarov, H. Leblond, and F. Sanchez, "Quintic complex Ginzburg-Landau model for ring fiber lasers," *Phys. Rev. E Stat. Nonlin. Soft Matter Phys.* **72**(2), 025604 (2005).
21. N. Akhmediev, J. M. Soto-Crespo, and G. Town, "Pulsating solitons, chaotic solitons, period doubling, and pulse coexistence in mode-locked lasers: Complex Ginzburg-Landau equation approach," *Phys. Rev. E Stat. Nonlin. Soft Matter Phys.* **63**(5), 056602 (2001).
22. A. Chong, J. Buckley, W. Renninger, and F. Wise, "All-normal-dispersion femtosecond fiber laser," *Opt. Express* **14**(21), 10095–10100 (2006).
23. D. Mortag, D. Wandt, U. Morgner, D. Kracht, and J. Neumann, "Sub-80-fs pulses from an all-fiber-integrated dissipative-soliton laser at 1 μm ," *Opt. Express* **19**(2), 546–551 (2011).
24. K. Ozgören, B. Öktem, S. Yilmaz, F. Ö. İlday, and K. Eken, "83 W, 3.1 MHz, square-shaped, 1 ns-pulsed all-fiber-integrated laser for micromachining," *Opt. Express* **19**(18), 17647–17652 (2011).
25. A. I. Chernykh and S. K. Turitsyn, "Soliton and collapse regimes of pulse generation in passively mode-locking laser systems," *Opt. Lett.* **20**(4), 398–400 (1995).
26. B. N. Nyushkov, V. I. Denisov, S. M. Kobtsev, V. S. Pivtsov, N. A. Kolyada, A. V. Ivanenko, and S. K. Turitsyn, "Generation of 1.7-uJ pulses at 1.55 μm by a self-mode-locked all-fiber laser with a kilometers-long linear-ring cavity," *Laser Phys. Lett.* **7**(9), 661–665 (2010).
27. B. N. Nyushkov, A. V. Ivanenko, S. M. Kobtsev, S. K. Turitsyn, C. Mou, L. Zhang, V. I. Denisov, and V. S. Pivtsov, "Gamma-shaped long-cavity normal-dispersion mode-locked Er-fiber laser for sub-nanosecond high-energy pulsed generation," *Laser Phys. Lett.* **9**(1), 59–67 (2012).

1. Introduction

All-normal dispersion fiber lasers mode-locked due to effect of nonlinear polarization evolution (NPE) are actively studied last year's being simple and efficient tool for ultra-short pulse generation. Compared to mode-lock lasers based on saturable absorbers this type of lasers has more robust and reliable design and tolerance to power damage. Compared to soliton generation in the anomalous group velocity dispersion (GVD) regime, use of the normal dispersion allows one to achieve higher pulse energies without wave breaking [1–3]. Further increase of pulse energy can be achieved due to cavity elongation. Since pulse repetition rate for mode-lock lasers is inversely proportional to cavity length, pulse energy grows linearly with cavity length if average generation power is fixed. Thus for example the paper [4] reports for the first time lasing in a hybrid (consisting of both bulk elements and fiber sections) 3.8-km-long mode-lock master oscillator with pulse energy as high as 3.9 μJ .

Recent experiments with all-normal-dispersion NPE mode-locked lasers both with short and long cavities show a large variety of lasing regimes [5] which can be divided into two types. The first is multi-pulse generation which several pulses co-exist in laser cavity at each moment [6,7]. The second regime which will be referred hereafter as single-pulse generation implies generation of only one pulse (which however may also comprise a series of sub-pulses) during cavity round-trip. This work is aimed to investigate features of single-pulse generation regimes of all-normal-dispersion NPE mode-locked lasers only. Let's note that in lasers of other types including oscillators mode-locked due to saturable absorbers (such as SESAM, single-wall nanotubes) as well as NPE-lasers with net normal dispersion single-pulse generation regimes may differ from those of ANDi NPE mode locked lasers [8–10].

As it was shown earlier in the case of single-pulse generation the lasers under consideration can generate pulses of different energy and duration and even qualitatively different pulses at fixed pump power and different settings of polarization elements [11]. Classification and understanding of lasing regimes is therefore important for optimal laser tuning. It was reported earlier single-pulse noise-like generation as well as stable bell-shaped pulse generation [11–15]. In the paper [16] authors pointed out four experimentally found generation regimes and proposed their classification based on super-continuum generation efficiency. This work investigates experimentally and with the use of numerical simulations three key single-pulse generation regimes of all-normal dispersion fiber lasers which differ from each other in temporal structure and pulse-to-pulse stability. A novel generation regime

which takes intermediate place between stable single-pulse generation and single-pulse noise-like generation is demonstrated in such lasers. A correlation between pulse-to-pulse stability, shape of spectrum and auto-correlation function (ACF) and pulse compressibility of laser pulses are shown for different generation regimes.

2. Laser scheme and numerical simulations

In our experiments we used the same Yb-doped fiber ring-cavity laser as in our previous paper (see [11] and Fig. 1). We used 7-m long active ytterbium fiber with a 7- μm core as the laser active medium and 1.5W pumping at 980 nm. For control of the polarisation state in the layout, two fiber-based polarisation controllers PC1 and PC2 were employed. For elongation of the laser cavity and boosting of the output pulse energy a stretch of passive SMF-28 fiber

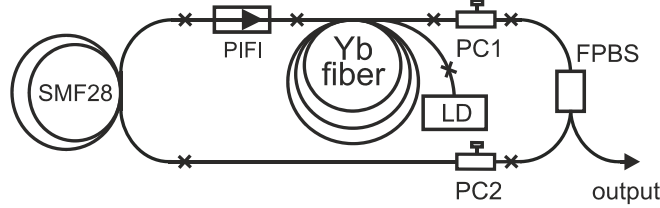


Fig. 1. Experimental laser scheme: PC - polarization controller, PIFI - polarization-independent fiber isolator, FPBS - fiber polarization beam splitter, LD - pump laser diode

was inserted, so that the full resonator length came to 11.2 m (round trip time $\tau = 54$ ns). All optical fibers in this layout had normal dispersion within the working spectral range of the laser. The average output power of the laser was limited by the power rating of fiber polarization beam splitter (FPBS) and did not exceed 150 mW. In order to have a deeper insight into experimental observations we simulate our laser using a standard approach based on the system of modified non-linear Schrödinger Eqs. (1), (2) [17]:

$$\frac{\partial A_x}{\partial z} = i\gamma \left\{ |A_x|^2 A_x + \frac{2}{3} |A_y|^2 A_x + \frac{1}{3} A_y^2 A_x^* \right\} + \frac{g_0/2}{1 + E/(P_{sat} \cdot \tau)} A_x - \frac{i}{2} \beta_2 \cdot \frac{\partial^2 A_x}{\partial t^2} \quad (1)$$

$$\frac{\partial A_y}{\partial z} = i\gamma \left\{ |A_y|^2 A_y + \frac{2}{3} |A_x|^2 A_y + \frac{1}{3} A_x^2 A_y^* \right\} + \frac{g_0/2}{1 + E/(P_{sat} \cdot \tau)} A_y - \frac{i}{2} \beta_2 \cdot \frac{\partial^2 A_y}{\partial t^2} \quad (2)$$

where A_x , A_y are the orthogonal components of the field envelope, z is a longitudinal coordinate, t – time, $\gamma = 4.7 \times 10^{-5} (\text{cm} \cdot \text{W})^{-1}$ – non-linear coefficient, g_0 – unsaturated gain coefficient, $\beta_2 = 23 \text{ ps}^2/\text{km}$ – dispersion coefficient, P_{sat} – saturation power for the active fiber, τ – time of cavity round trip. In our calculations we neglected the higher-order dispersion and linear bi-refringence of the fiber. For simplification of the analysis and reduction of the required computation resources we shortened the laser cavity to 10 m in our calculations. The amplifier parameters were estimated from experimental measurements and taken equal to $g_0 = 540 \text{ dB/km}$, $P_{sat} = 52 \text{ mW}$. Since our goal here is a qualitative analysis of different lasing regimes rather than seeking exact match between experiment and simulations, some possible inaccuracy of laser parameters does not affect the main results. In particular we checked that qualitatively the same regimes can be found in simulation with considerably different values of cavity length, dispersion, gain and saturation power.

To improve convergence of the solution to the limiting cycle, the numerical modelling included a spectral filter with a 30-nm band-width, which exceeds considerably the typical width of generated laser pulses. In experiments implicit spectral filtering is performed by wavelength-dependent gain of the active fiber as well as effective Lyot filter action of optical

fiber and FPBS [18,19]. The effect of polarisation controllers was taken into account by introduction of corresponding unitary matrices (see e.g [11,20].).

Equations (1), (2) were integrated numerically using step-split Fourier method. White noise (1 photon per each mode with random phases) was used as initial conditions. In the most cases the laser needs less than 500 round-trips to enter the regime. As a rule we simulated pulse propagation over 5×10^3 successive cavity round-trips but in order to confirm stability of selected regimes we inspect pulse evolution over 10^5 round-trips. We also checked that changing neither mesh width nor integration step affected the results of our simulations. The most of stable lasing regimes could be reproduced after any reasonable change of those parameters and initial conditions. As for noise-like and intermediate regimes they could be reproduced only qualitatively and by means of their averaged characteristics due to their stochastic nature. Note that for some PC settings both stable and noise-like generation could be obtained depending on random realization of initial noise similar to reported in [21].

3. Results and discussion

The results of our experiments and numerical simulations show that ANDi lasers support a large variety of generation regimes which can be hot-switched by changing PC settings. Laser pulses generated at different PC settings may have different energy, duration, shape and width of spectrum. Another important difference between generation regimes is a pulse-to-pulse stability. The latter affects significantly pulse compressibility what is critical for many applications of ultra-fast lasers with large normal cavity dispersion. Moreover pulse-to-pulse stability determines lasing spectrum which can be either frequency comb or smooth continuum spectrum what is essential for metrological applications of such lasers and super-continuum generators on their basis.

Our numerical study shows that a whole series of generation regimes are extremely stable and have parameters fluctuations as small as $10^{-6} \dots 10^{-4}$. Bell-shaped ACF and Π -shaped spectrum with steep edges are distinctive features of stable generation regime, see left graphs in Fig. 2. Note that spectral edges are steep even in logarithmic scale of spectral power what is corroborated both with numerical simulations and experiments.

A principally different generation regime from the point of view of pulse-to-pulse stability which also can be easily realized in ANDi NPE mode-locked lasers at different settings of PC or/and different pump power is a single-pulse noise-like generation [12–15]. In this regime laser generates wave packets with complex temporal structure comprising a set of sub-pulses [11]. Integral characteristics of whole wave packet such as energy and duration fluctuate slightly around their average exhibiting typical alteration of several percent. At the same time the inner temporal structure of the wave packet changes dramatically demonstrating noise-like behavior what makes them somewhat similar to chaotic solitons [21]. However, in contrast to chaotic solitons, noise-like pulses have complex temporal structure being a set of sub-pulses what relates it to exploding solitons in the stage of “lava” [21]. In contrast to exploding solitons noise-like pulses demonstrate neither pulsations nor returns to bell-shaped pulses. Noise-like pulses have two different scales of time coherence: the duration of whole wave packet and duration of constituent sub-pulses. The presence of two time scales can be readily seen in ACF obtained both in experiments and numerical simulations, see Fig. 2, right graphs. Smooth spectrum and ACF pedestal appear as a result of time average over consequent pulses whereas both spectrum and ACF of a single wave packet are indented [11].

A detailed study performed in this work shows that novel intermediate regimes do exist between the aforementioned two types of lasing. Laser pulses generated in this regime are hybrid between stable and chaotic pulses that combines complex chaotic dynamics with self-organization at each moment what differs it from e.g. soliton explosion regime [5]. Spectra generated in such regimes have steep edges with smooth slope at the bottom. ACF of such pulses has typical double-scale structure with tiny peak on a high pedestal. In other words both spectrum and ACF registered in such intermediate regime have transitional shape

between those observed in stable and noise-like single-pulse generation regimes, see Fig. 2 in the middle. Let's note that ACF pedestal may have different shapes depending on PC settings. In particular we observed in numerical modeling ACFs with quasi-triangular profile [16] however such ACFs contained a femtosecond peak on the triangular pedestal indicating stochastic nature of generation regime.

Good qualitative agreement between numerical simulations and experiments in ACF and spectra for all three types of lasing shown in Fig. 2 allows us to use numerical modeling to get a deeper insight into features of generation regimes. Thus Fig. 3 shows simulated temporal dependences of pulse phase $\varphi(t)$ and frequency shift $\Delta\nu = -(\text{d}\varphi/\text{d}t)/(2\pi)$. Experimental measurement of optical phase is quite complex especially in the case of stochastic generation where single-pulse measurement techniques must be used.

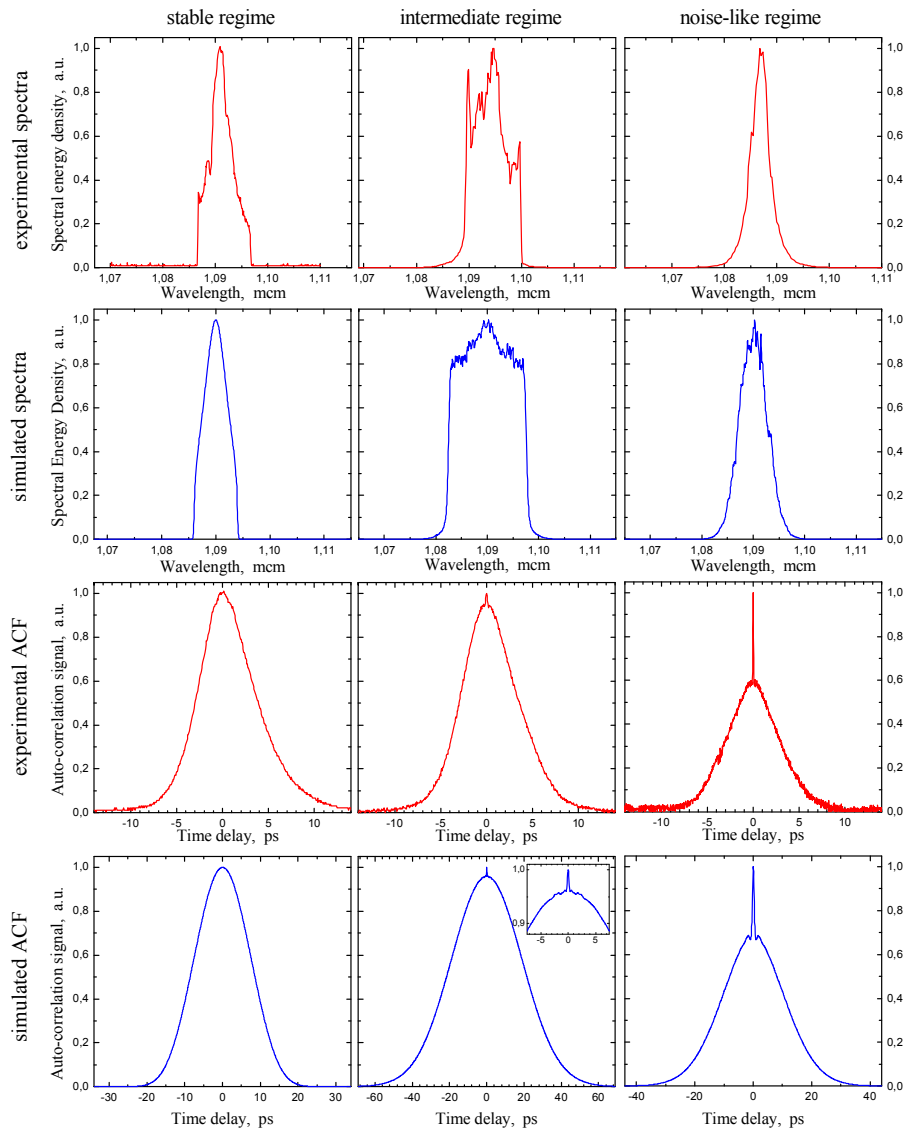


Fig. 2. Experimentally measured (red) and simulated (blue) spectra and ACFs for three different lasing regimes: stable single-pulse (left column), intermediate (middle column) and noise-like generation (right column).

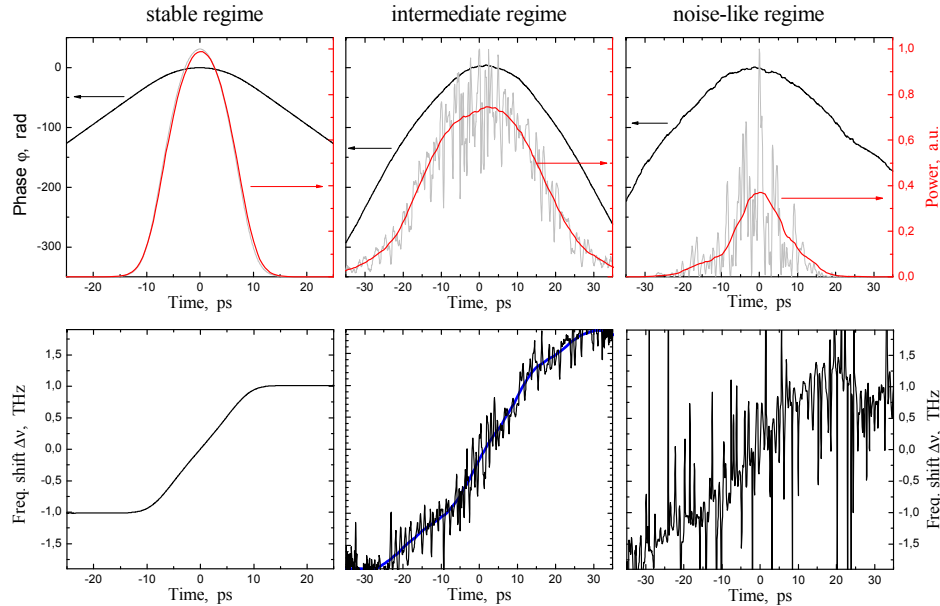


Fig. 3. Simulated time dependences of pulse power and phase (upper graphs) and frequency shifts (lower graphs) for three different lasing regimes.

It can be seen in Fig. 3 that optical pulse generated in stable single-pulse regime has smooth bell-shaped temporal profile shown with grey and red lines in the top-left graph in Fig. 3. Phase profile of such pulse is parabolic at pulse center (black line) what corresponds to nearly linear chirp (see bottom-left graph in Fig. 3). This makes possible highly efficient temporal compression virtually down to Fourier limit what agrees well with experimental observations made by us and other authors [22,23]. Temporal intensity profile $I(t)$ in the intermediate generation regime shown in grey on the middle-top graph in Fig. 3 looks like a “noisy” pulse, i.e. stochastic intensity oscillation about bell-shaped envelope shown in red. Let’s note that the amplitude of these oscillations is much less than its average value so that $I(t)$ doesn’t fall to zero at the pulse center. Similar to stable single-pulse generation, temporal phase dependence $\varphi(t)$ in the intermediate generation regime has parabolic form with a tiny high-frequency fluctuations that are almost invisible. However after derivation the fluctuation grow considerably so that linear chirp in the intermediate regime is noticeably disturbed, see black line on the middle-bottom graph in Fig. 3. The blue line shows smoothed frequency shift $\Delta v(t)$ which is nearly linear at the pulse center. These frequency fluctuations limits pulse compressibility which can be estimated as follows. Let’s express frequency shift $\Delta v(t)$ as $\alpha v + \delta v(t)$, where $\delta v(t)$ is stochastic fluctuations and α denotes average slope proportional to average pulse chirp and can be estimated as $\Delta v/T_0$, where Δv is the width of spectrum and T_0 stands for pulse duration. A prism or grating compressor performs transformation $t \rightarrow t' = t - v/\alpha$, after that pulse duration can be estimated as $T' = T_{sp,lim.} + 2T_0|\delta v|/\Delta v$, where $T_{sp,lim.}$ denotes duration of Fourier-limited pulse. In the presence of considerable chirp fluctuations the second term prevails so that resulting compression ratio can be estimated as simple as $k = T_0/T' \sim \Delta v/|2\delta v|$. Substituting intermediate generation regime parameters (see Fig. 3): spectral width $\Delta v \sim 3.8$ THz ($\Delta\lambda \sim 15$ nm), frequency fluctuations $|2\delta v| \sim 1$ THz we obtain $k \sim 3.8$. Numerical modeling yields compression ratio $k = 4.75$ what has the same order of magnitude. (Let’s note for comparison that maximum pulse compression ratio would be two orders of magnitude greater if there were no frequency fluctuations since $T_0/T_{sp,lim.} \sim 300 \dots 400$ depending on pulse shape.) This result is also in a reasonable agreement with our experimental observations. Thus compression ratio about 3.5 is achieved experimentally for

laser pulses which have double-scaled ACF with a tiny femtosecond peak on a picosecond pedestal. In other words temporally compressed pulses generated in the intermediate lasing regime are far from Fourier limited.

Finally, in the third (stochastic) generation regime the pulse looks like a noise-like wave-packet consisting of a series of femtosecond sub-pulses. The intensity of this wave-packet falls down to zero throughout the pulse. Temporal phase profile $\phi(t)$ is close to parabolic with clearly seen high-frequency fluctuations. Frequency $\Delta\nu(t)$ demonstrates strong fluctuations with amplitude comparable or even greater than spectral width what corresponds to experimentally measured random chirp [24]. Using estimation for maximum pulse compression ratio obtained above we obtain $k \sim \Delta\nu/|2\delta\nu| \sim 1$ what means that noise-like pulses are not compressible and agrees with results of our experiments and modeling.

Up to the present there's a lack of simple qualitative explanation of physical mechanisms involved in noise-like and intermediate generation regimes. Earlier it was supposed that noise-like generation is caused by polarization-dependent delay effect [12], however in our work there's no linear birefringence. Based on a similar model as we used, Tang *et al* [14] arrived at a conclusion that the key physical reason of noise-like generation is the soliton collapse effect [25]. However it's not apparent even when number of noise-like sub-pulses is quite moderate. Moreover we observed also some other patterns of pulse behavior e.g. one similar to reported in [21] when chaotic sub-pulses are formed at pulse center and then move towards pulse edges and disappear there most likely due to self-amplitude modulation resulted from combined action of PBS and NPE. However we confirm the previously observed fact [11,14] that when the laser switches to noise-like generation regime in the course of adiabatic change of cavity settings (such as PC settings or pump power) the laser cavity feedback becomes positive due to specific transmission function of NPE-based laser cavity. The pulse amplitude starts to grow at that moment and the pulse decays shortly into a series of sub-pulses. Another conclusion that can be made on the basis of our observations is that in relatively long cavities the laser tend to stochastic regimes rather than to stable ones. The latter fact is usually referred as NPE overdriving and resulted from non-monotonic power dependence of NPE-based artificial saturable absorber. That's why extremely long NPE-based lasers show multi-pulse operation or produce noise-like pulses with smooth bell-shaped spectra [4]. Since NPE overdriving is a quite general effect one can expect noise-like or intermediate (semi-chaotic) generation also for ultra-long NPE-based lasers with anomalous dispersion and dispersion-mapped cavities [26,27].

4. Conclusion

Thus both experimentally and with the use of numerical simulations this work demonstrates novel single-pulse generation regimes that take intermediate place between well-known stable single-pulse generation and noise-like single-pulse generation in all-normal-dispersion NPE mode-locked fiber lasers. The unique features of novel regime which make it possible to identify this regime in experiments are double-scaled ACF with a tiny femtosecond peak on a picosecond pedestal and optical spectrum with steep edges with smooth slope at the bottom. Pulse intensity contains high-frequency jitter however it generally doesn't fall to zero within optical pulse in contrast to noise-like generation regime. Optical phase also fluctuates what results in temporal jitter of instantaneous frequency and limits considerably compression ratio of such pulses.

Acknowledgments

This work was partially supported by the Council of the President of the Russian Federation for the Leading Research Groups of Russia, project No. NSh-2979.2012.2; Marie-Curie International Exchange Scheme, Research Executive Agency Grant "TelaSens" No 269271; Grants of Ministry of Education and Science of the Russian Federation (agreement No. 14.B37.21.0452; project No. 01200907579)